RSC Advances

ROYAL SOCIETY OF CHEMISTRY

www.rsc.org/advances

RSC Advances

ARTICLE

Controlling the Morphology and Property of Carbon Fiber/Polyaniline Composites for Supercapacitor Electrode Materials by Surface Functionalization

Received 00th January 20xx,
Accepted 00th January 20xx

DOI: 10.1039/x0xx00000x

www.rsc.org/

Fuyou Ke,[a] Jun Tang,[a] Shanyi Guang[b] and Hongyao Xu[a]

The effect of surface functionalization of carbon materials on the morphology and performance of carbon/polymer composite materials for supercapacitor electrodes was investigated here. Three kinds of functionalized carbon fibers were prepared by the simple chemically modification of carbon fiber, named oxidated carbon fiber (OCF), amino-functionalized carbon fiber (AFCF) and aminated triazine functionalized carbon fiber (ATFCF). Then functionalized carbon fibers were used to fabricate nanostructural polyaniline/CFs composites (PANI/OCF, PANI/AFCF, PANI/ATFCF) by electrochemical in-situ polymerization under pulse current. The chemical compositions and morphologies of these PANI/CFs composites were studied by FTIR, Raman spectra and SEM. It was found that PANI on OCF composites displayed disordered nanofiber structure owing to the non-covalent connection between PANI with OCF. Conversely, PANI grew on the surface of AFCF and ATFCF in an ordered fashion due to chemically covalent connection, exhibiting nanowire arrays and petal-like nanosheets, respectively. It hints that the morphology of PANI/CFs composites can be effectively adjusted by molecular structural design of functional groups on the functionalized CF. The electrochemical properties of these PANI/CF composites were evaluated by electrochemical workstation. In comparison with noncovalent PANI/OCF composites, the strong covalent interactions together with the ordered nanostructures of PANI/AFCF and PANI/ATFCF facilitated faster charge transfer, smaller internal resistance and better mechanical properties, resulting in improved electrochemical performance.

1. Introduction

The correlation between structure and performance is a concern in material science, because studies on their relationship are helpful in understanding the related mechanisms, designing novel structures to prepare the materials with ultra-performance and predicting the properties of new materials. Carbon based composite materials have been attracting much attention in the past years. Their performance strongly depends on the hierarchy structures and the interactions between their components. Because of the inert surface of carbon materials, their interactions with the other components (e.g. polymers) are very weak, deteriorating the performance of composite materials, thus carbon materials require surface functionalization to enhance the interactions with other components. When the simple in situ polymerization method is used to prepare carbon/polymer composite materials, surface functionalization of carbon materials not only improves the interactions, but also guides the growth of polymers to form various morphologies, further affecting the performance of the composite materials. Thus studies on the relationships between functional groups, morphologies and performance are very significant in the field of carbon/polymer composite materials. In this paper, such studies were conducted in the application of supercapacitor electrode materials.

Supercapacitor is a new high-performance energy storage device with ultrahigh power density, fast charge-discharge rate, long cycle life, and low maintenance cost. According to its mechanisms named electrical double layers capacitance and pseudocapacitance, the electrode materials can be divided into two categories, respectively. The former are carbon-based materials[1-2], such as graphene, carbon nanotube and carbon fibers. They have good mechanical properties and cycling stability, but low capacitance. The latter are mainly conductive polymers[3] and metal oxides. They display high capacitance but poor cycling stability. Thus, the recent studies in high performance supercapacitor focus on the composite electrode materials integrating high capacitance and good cycling stability.

[a]State Key Laboratory for Modification of Chemical Fibers and Polymer Materials, College of Materials Science and Engineering, Donghua University, Shanghai 201620, P.R. China. E-mail: hongyaoxu@163.com; Tel: +86-21-67792228
[b]College of Chemistry & Chemical Engineering, Donghua University, Shanghai 201620, P. R. China. E-mail: syg@dhu.edu.cn; Tel: +86-21-67792874
Electronic Supplementary Information (ESI) available: FTIR spectra and Raman spectra of PANI and PANI/CF composite materials; Specific capacitance of CFs at various current densities. See DOI: 10.1039/x0xx00000x

Polyaniline (PANI) is one of the most promising conductive polymers in supercapacitor electrode materials owing to its easy synthesis, low cost and high capacitance. Compared with the macroscopic PANI, the nano structures of PANI significantly improve the electrochemical performance. Various morphologies of PANI[4-5], such as spheres[6], tubes[7] and nanowires[8], were designed and fabricated by using different synthesis methods, including oxidative polymerization and electrochemical polymerization. To overcome the poor cycling stability problem of conductive polymers as described above, PANI based composite electrode materials were widely studied[9], mainly focusing on PANI/carbon based composite materials[10-18]. In our recent work, highly ordered PANI nanorods array/graphene bulk hybrid materials were prepared for high performance supercapacitor electrodes, which possess a specific capacitance as high as 1225 F g^{-1} at 1 A g^{-1}, together with outstanding rate capability and cycling stability because of the synergistic effect[19].

In comparison with other carbon based materials, carbon fibers (CF) display characteristic merits, e.g. low cost and the absence of aggregation problem like graphene, high strength and excellent flexibility, which make carbon fibers to be very promising in the applications of flexible supercapacitors. Thus PANI/CF composite electrode materials have been prepared in many groups[20] and they show both high capacitance and good cycling stability. Yan et al.[21] and Liu et al.[22] fabricated free-standing, flexible PANI/CF paper composite materials via in-situ polymerization of aniline, respectively. Cheng et al. prepared PANI/CF composite electrode materials by coating PANI nanowires onto the electro-etched CF cloth, which reach a mass-normalized specific capacitance of 673 F/g and an area-normalized specific capacitance of 3.5 F/cm2[23]. Yu et al. further improved the electrochemical performance by using nitrogen plasma etching[24-25]. Because of the inert surface, functionalized CF was supposed to enhance the interactions between PANI and CF. It has proved that the covalent linkage can facilitates charge transfer, and consequently improves capacitance and cycling ability in the composite materials[26], which requires the surface functionalization of CF. However, there are few reports on the chemical modification of CF for PANI/CF composite materials as supercapacitor electrodes except the etching techniques. On the other hand, structural design of functional groups on CF surface can be used to adjust the PANI growth and morphologies, especially when in situ polymerization method is adopted, further controlling the performance of PANI/CF composite materials in supercapacitor electrodes. However, the effect of surface functionalization of CF on the PANI morphology and the resulting performance of PANI/CF composite materials in supercapacitor electrodes has not been investigated.

Here three kinds of functionalized carbon fibers were prepared by the chemical modification of carbon fiber, named oxidated carbon fiber (OCF), amino-functionalized carbon fiber (AFCF) and aminated triazine functionalized carbon fiber (ATFCF). Then three different nanostructural PANI/CFs composites (PANI/OCF, PANI/AFCF, PANI/ATFCF) were fabricated based on functionalized carbon fibers (OCF, AFCF, ATFCF) by electrochemical in-situ polymerization under pulse current, as shown in **Figure 1**. The chemical compositions, morphologies, and electrochemical performances of PANI/CFs were investigated and their relationships were discussed.

2. Experimental

2.1 Materials

T700 carbon fiber was purchased from Toray. Concentrated sulfuric acid (H_2SO_4, 98%), hydrochloric acid (HCl), sodium bicarbonate ($NaHCO_3$), p-phenylenediamine, N, N-dimethylformamide (DMF), acetone and sodium nitrite ($NaNO_2$) were purchased from Shanghai Reagent Company. Hydrazine hydrate (98%) was purchased from Alfa Aesar Company. 2,4,6-trichloro-1,3,5-triazine was obtained from J&K Company. Aniline (AR) was bought from Sinopharm Chemical Reagent Company, which was purified by vacuum distillation twice before use. Other chemical reagents were used directly without any further purification.

2.2 Preparation of PANI/CFs composite materials

2.2.1 Pre-treatment of CF

0.36 g CF was wound in parallel with 25cm-long glassy shelves, and then immersed in 100 mL acetone at room temperature for 4 hours. After that, CF was washed with deionized water for three times and dried in blast oven at 85 ℃ for 24 hours until the weight is constant, then CF was kept in a desiccator before use.

2.2.2 Synthesis of oxidized carbon fiber (OCF)

OCF was obtained via electrochemical oxidation method. 60 mg CF was wound with plastic plate, used as the anode and two sheets of copper as the cathode. At a current density of 4.5 A/g, the electrolysis was conducted in 200 mL 3wt% NH_4H_2PO4 electrolytes for 30 min. Then OCF was washed with deionized water and dried in blast oven at 85 ℃

2.2.3 Synthesis of amino-functionalized carbon fiber (AFCF)

AFCF was obtained through diazonium salt addition reaction between carbon fiber and p-phenylenediamine. First, a three-necked flask was charged with 200 mg OCF and 200 mL deionized water, then 0.6 mL 98% hydrazine hydrate was added under stirring. The solution was refluxed at 100 ºC for 4 h, then 3 mL 12 M HCl was added to form an acidic environment. After that, 0.1226 g of *p*-phenylenediamine and 0.0266 g $NaNO_2$ were added and kept in an ice bath for 2 h under stirring. The product was washed repeatedly with acetone, DMF and deionized water, then dried in a vacuum oven at 50 ºC.

RSC Advances

ARTICLE

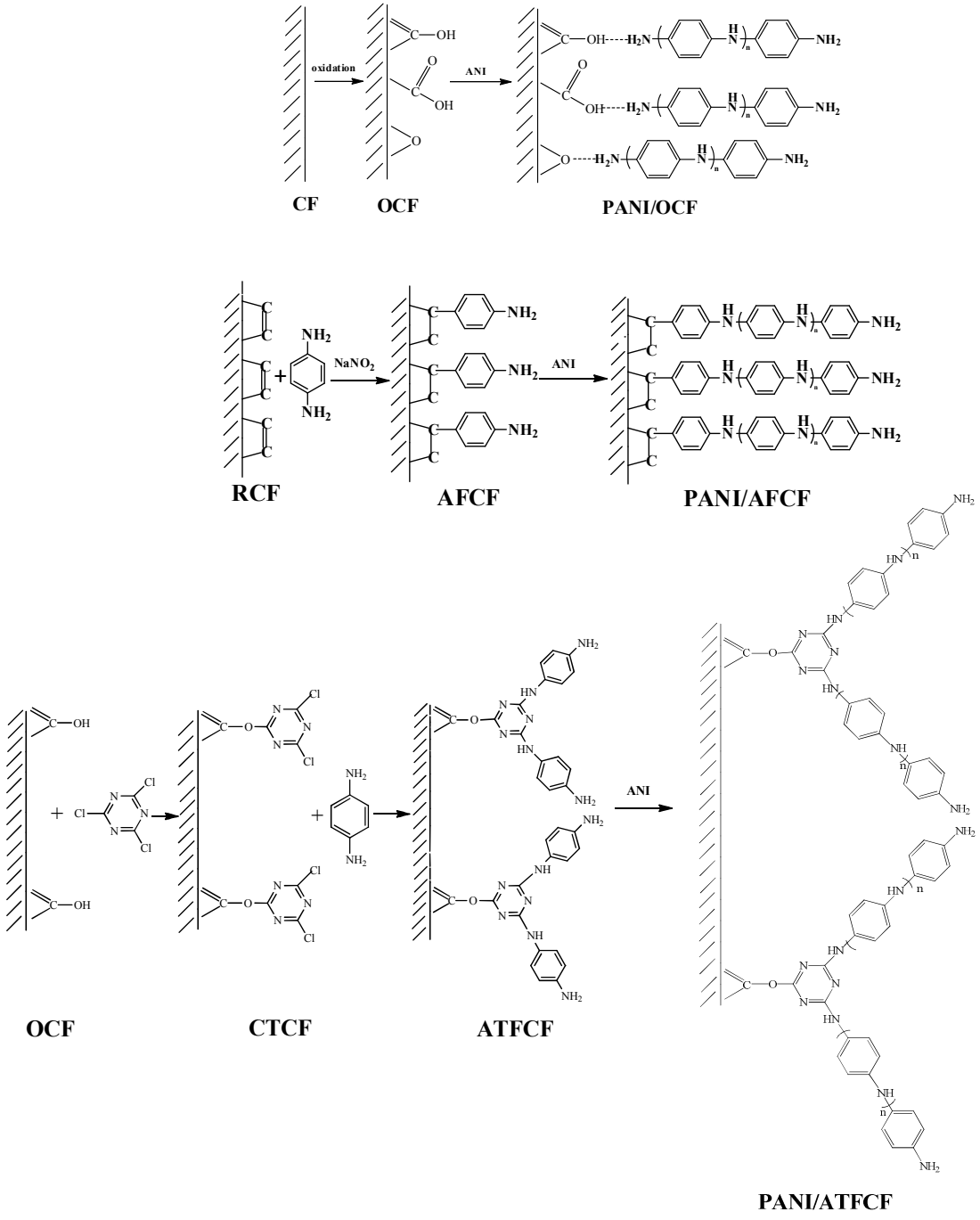

Figure 1 Schematic illustration of the preparation of PANI/OCF, PANI/AFCF and PANI/ATFCF composite materials.

RSC Advances

ARTICLE

2.2.4 Synthesis of aminated triazine functionalized carbon fiber (ATFCF)

A round bottom flask was charged with 200 mg OCF, 2.73 g $NaHCO_3$ (32.5 mmol) and 120 mL DMF in an ice bath. 1.5 g (8.13 mmol) 2,4,6-trichloro-1,3,5-triazinewas dissolved in DMF and added dropwise to the above solution. The solution was further stirred for 4 h. Then 3.516 g (32.52 mmol) p-phenylenediamine was added under nitrogen atmosphere. The mixture was first stirred at room temperature for 4 h, then refluxed for 24 h at 90ºC. The product was washed repeatedly with acetone, DMF and deionized water, then dried in a vacuum oven at 50 ºC.

2.2.5 Synthesis of PANI/CFs composites

PANI/CFs composite materials were all prepared via electrochemical polymerization of aniline under pulse current. In a typical procedure, 60 mg OCF were wound with plastic plate, used as the anode and two sheets of copper as the cathode. At a current density of 6 A/g, the electrochemical oxidation was conducted in 200 mL 0.3 M ANI + 1.0 M H_2SO_4 electrolytes for 7 min with 50% duty cycle. Then the composite materials were washed with deionized water and dried in vacuum oven at 60 ℃, which are named as PANI/OCF. Similarly, the other composite materials from AFCF and ATFCF are named as PANI/AFCF and PANI/ATFCF, respectively. For good comparison, the composite materials from unmodified CF were also prepared and named PANI/CF below. The weight percentage of PANI in PANI/CF, PANI/OCF, PANI/AFCF and PANI/ATFCF were calculated as 22.2%, 26.5%, 29.8% and 30.8%, respectively.

2.3 Characterization

FTIR spectra were recorded in the region of 4000-500 cm^{-1} on a Nicolet NEXUS 8700 FTIR spectrophotometer using KBr disks at room temperature. Raman spectra were recorded using a Via-Reflex Micro-Raman spectroscopy (Renishaw). The morphologies of PANI/CF composite materials were observed with a field-emission scanning electron microscope (FESEM, Hitachi S-4800). Electrochemical measurements were carried out in a three electrode system. The composite materials were directly used as the working electrodes. A platinum sheet ($1\times1cm^2$) and a Ag/AgCl with saturated KCl solution were used as the counter and the reference electrode, respectively. Cyclic voltammetry (CV) and galvanostatic charge-discharge (GCD) were measured using a CHI660D electrochemical workstation at room temperature. The electrochemical impedance spectra (EIS) were performed using a ZahnerZennium electrochemical workstation. An aqueous solution of 1 M H_2SO_4 was used as the electrolyte. CV tests were carried out from 0 to 0.8 V at different scan rates from 10-500 mV/s. The GCD property was measured at current densities from 1 to 8 A g^{-1}. Measurement of cycling stability was performed by cyclic voltammetry at a scan rate of 100 mV s^{-1}. The EIS were obtained at the open circuit voltage with an applied amplitude of 5 mV for swept frequencies of 0.01–100 kHz. The specific capacitance values (Cs, F g^{-1}) of the samples were calculated from the discharge process according to the following equation:

$$C_s = I \times \Delta t / (\Delta V \times m)$$

where I is the charge–discharge current (A), Δ t is the discharge time (s), Δ V is the potential change during the discharge process and m is the mass of active material in a single electrode (g).

3. Results and Discussion

Three kinds of chemically modified CFs including OCF, AFTF and ATFCF were designed here and their composite materials PANI/OCF, PANI/AFCF, PANI/ATFCF were prepared via electrochemical polymerization of aniline. As shown in **Figure 1**, CF and PANI were connected through hydrogen bonding in PANI/OCF, while covalent connections existed in the other two composite materials.

Figure 2 shows FTIR spectra and Raman spectra of the functionalized CFs. In the FTIR spectrum of OCF, the absorption bands at 3464, 1726, 1604, 1246, 1044 cm^{-1} were attributed to the stretching vibrational peaks of -OH, C=O, C=C, -C-OH, -C-O-C, respectively, indicative of the oxidation of CF surface. The characteristic absorption bands of stretching vibrational peaks of $-NH_2$ occurred at 3423 and 3468cm^{-1} in the FTIR spectra of both AFCF and ATFCF. Moreover, the absorption bands at 1564, 1456 and 1334 cm^{-1} came from the triazine skeleton. These results proved the successful functionalization of CF. Raman spectra were used to study the structural variation of CFs after functionalization. As shown in **Figure 2B**, CF had two absorption peaks at 1604 and 1346 cm^{-1}, corresponding to the G band and D-band, originating from the ordered (sp2 hybridized carbon) and disordered graphite structure. The intensity ratio of G-band to D-band I_G/I_D of initial CF was 0.96. After modification, I_G/I_D increased to 1.05 in OCF, 1.10 in AFTF and 1.14 in ATFCF, suggesting a larger conjugated structure because of the incorporation of oxygen or nitrogen atoms on the surface.

RSC Advances

ARTICLE

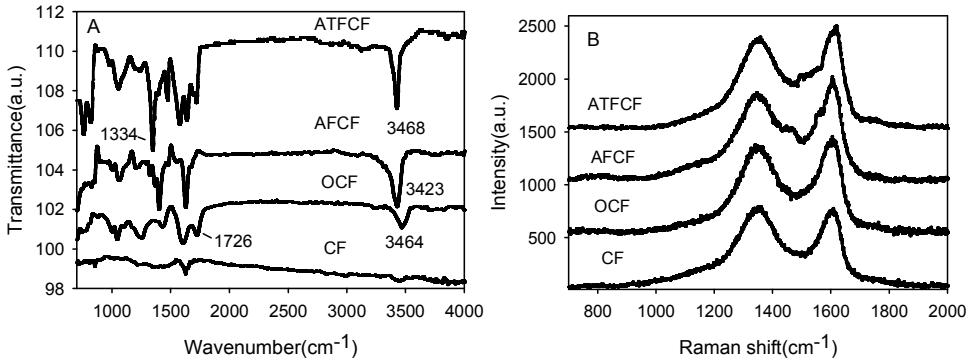

Figure 2 (A) FTIR spectra and (B) Raman spectra of CF and functionalized CFs.

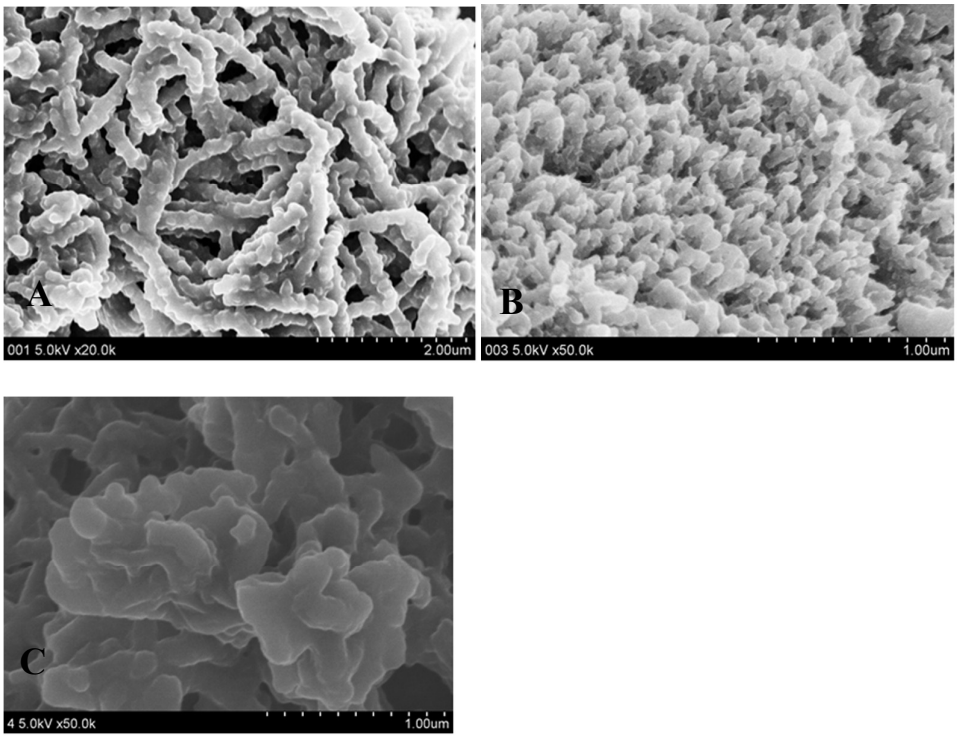

Figure 3 SEM images of PANI/CFs composites. (A) PANI/OCF; (B) PANI/AFCF; (C) PANI/ATFCF.

PANI had two characteristic absorption bands at 1555 and 1467cm^{-1} in FTIR spectra (**Figure S1A**), corresponding to the stretching vibration of C=C in quinone rings and benzene rings. After PANI was coated to functionalized CF via in-situ polymerization of aniline, similar absorption bands were also observed in the spectra of composite materials, but with a red shift (PANI/OCF: 1545, 1454 cm^{-1}; PANI/AFCF: 1543, 1456 cm^{-1}; PANI/ATFCF: 1537, 1443 cm^{-1}), indicating that conjugated interactions existed between functionalized CF and PANI, while the interactions were strongest in PANI/ATFCF. In addition, the stretching vibrational bands of -NH_2 in AFCF and ATFCF disappeared in the composite materials, indicative of the

covalent connections between CF and PANI. The conjugated interactions were further confirmed by Raman spectra (**Figure S1B**). I_G/I_D of the composite materials further increased to 1.19 in PANI/OCF, 1.23 in PANI/AFCF and 1.24 in PANI/ATFCF. The morphologies of the composite materials were investigated by SEM. As shown in **Figure 3**, PANI on the PANI/OCF surface exhibited nanofibrous structure, but not ordered. While in PANI/AFCF composites, PANI formed nanowire arrays vertical to the CF surface. Different from the above, PANI in PANI/ATFCF composites showed petal-like sheet nanostructures. The variation in the PANI morphology of the composites was attributed to the difference in the functionalization of CF, which guided the growth of PANI on their surface. In PANI/OCF composites, there were no covalent connections between CF and aniline, only weak hydrogen bonding interactions existed. Thus the guiding role in PANI growth was very poor, resulting in disordered nanofibers Similar phenomenon was observed in PANI/CF, as shown in Figure S2. While in PANI/AFCF and PANI/ATFCF composites, the amino groups on the surface initiated the polymerization of aniline and guided the growth of PANI along the amino directions, thus ordered nanostructures were obtained. The different morphologies between PANI/AFCF and PANI/ATFCF originated from the distribution of amino groups on CF surface. The detailed formation mechanism of the petal-like nanoribbons can be seen in our further work. The above results suggested that the morphologies of PANI/CF hybrid materials strongly depended on the structural design of functional CF. Strong covalent connections between CF and PANI were inclined to form ordered structures, while the distribution of functional groups (amino groups here) guiding the PANI growth controlled the PANI morphology.

The electrochemical performances of PANI/CFs composite materials used as the supercapacitor electrodes were investigated using CV, GCD and EIS measurements. As shown in **Figure 4A**, the CV curves of PANI and PANI/CFs composites displayed two pairs of redox peaks (C1/A1 and C2/A2), which were attributed to the transition of PANI between a semiconducting state (leucoemeraldine form) and a conducting state (polaronicemeraldine form) and the Faradaic transformation from emeraldine to pernigraniline[12]. Because the capacitance of the samples was proportional to the area of CV curves, the capacitance of PANI/CFs composites mainly came from Faradaic reactions of PANI at the electrode/electrolyte surface. The areas of the CV curves of the composites were larger than that of PANI, indicating that the introduction of CF efficiently improved the capacitance. Moreover, the capacitances of PANI/functionalized CF composites were larger than that of unmodified CF, while the values were in the order: PANI/ATFCF>PANI/AFCF>PANI/OCF. At high scan rates, the CV curves of the composites (Figure 4B just shows the data of PANI/ATFCF, others are the same) were similar to those at low rates, the two pairs of redox peaks were still clearly observed, indicating that the composites had good capacitance response, mainly because these electrode materials had a high charge transfer rate. The good linear relationship between the anode current and scan rate (inset in **Figure 4B**) revealed that the composite electrode materials had excellent reversible stability and fast response to large current, which was beneficial in charge-discharge process at high power densities. **Figure 4C** shows the GCD curves of CF, PANI and their composites with a potential window from 0 to 0.8 V at a current density of 1 A g^{-1}. The specific capacitance (Cs, F g^{-1}) of the samples can be calculated from the discharge process according to the equation in Experimental part. The specific capacitance of PANI, PANI/CF, PANI/OCF, PANI/AFCF, PANI/ATFCF were calculated as 208.13, 322.95, 343.65, 406.14 and 456.73 F g^{-1}, respectively. The capacitance of the covalently grafted PANI composites (PANI/AFCF and PANI/ATFCF) was significantly greater than that of the non-covalent composites (PANI/OCF, PANI/CF). **Figure 4D** shows the dependence of the specific capacitance on the charge-discharge current density. The capacitance decreases with increasing the current density, because the rate of redox reaction and charge diffusion cannot match the rapid increase in current densities[27]. When the current density increased from 1 to 8A g^{-1}, the specific capacitances of PANI/CF, PANI/OCF, PANI/AFCF, PANI/ATFCF kept 47.80%, 49.71%, 50.49% and 50.92% of their initial values, much larger than that of PANI(28.31%) because of the synergistic effect. These results demonstrated that the four composites had good rate capacity, which was very important for the electrode materials of supercapacitor to provide high power density. In addition, PANI/functional CF composites exhibited better performance than PANI/CF, covalently grafted PANI composites (PANI/AFCF, PANI/ATFCF) exhibited better performance than non-covalent PANI composites (PANI/OCF), indicative of the importance of CF functionalization.

RSC Advances

ARTICLE

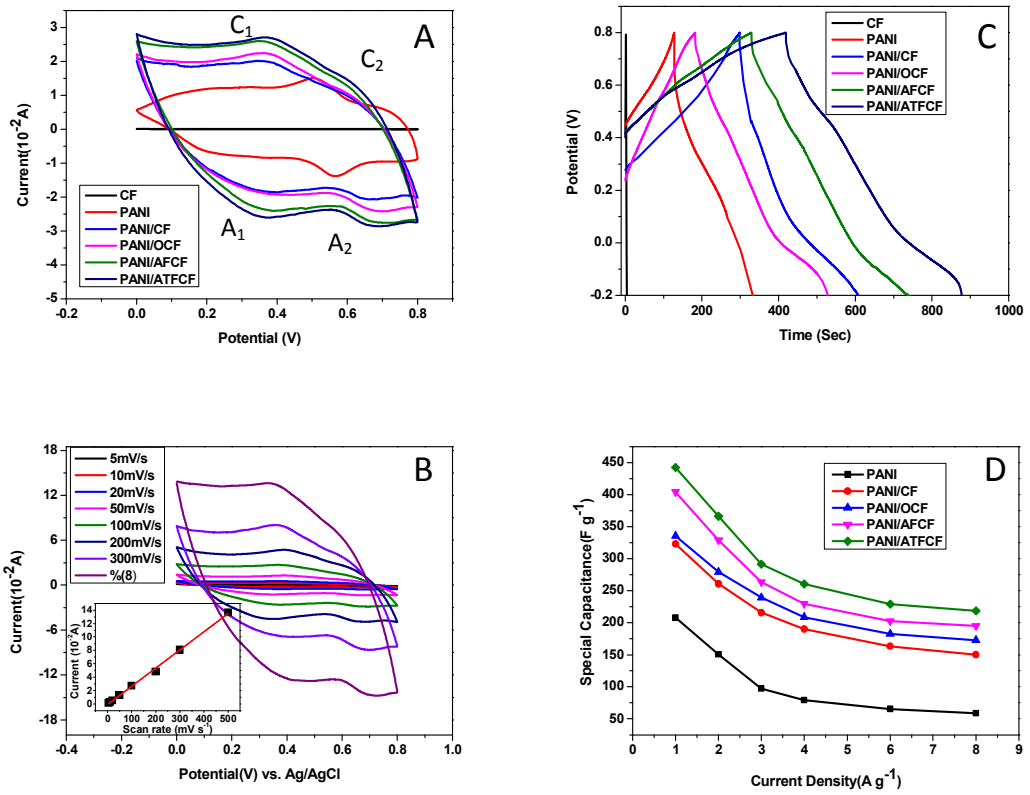

Figure 4 Electrochemical properties of PANI/CFs composite materials. (A) Cyclic voltammograms of samples at a scan rate of 100 mV s-1in 1 M H_2SO_4. (B) Cyclic voltammograms of PANI/ATFCF at various potential scan rates from 5 to 500 mV s^{-1}. (C) Charge and discharge curvesat a current density of 1 A g^{-1}. (D) Specific capacitance at various current densities.

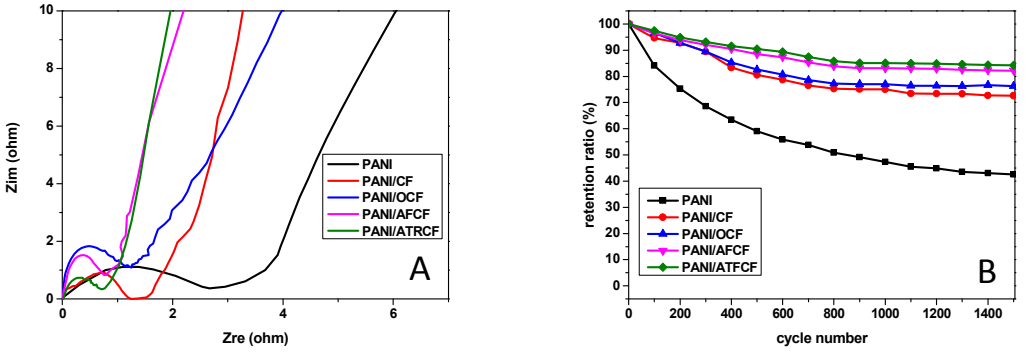

Figure 5 (A) Nyquist plots of PANI/CFs composite electrodes in the frequency range of 100 kHz to 0.01 Hz; (B) Cycling stability of PANI/CFs composite electrodes at 100 mV s^{-1} for 1500 cycles.

RSC Advances

ARTICLE

EIS was used to analyze the internal resistance, charge transfer kinetics and ion diffusion process. As seen in **Figure 5A**, the Nyquist curve of PANI at the high frequency region had a large semi-circle, and the interfacial charge transfer resistance R_{ct} was about 2.89Ω. While the composites materials showed the negligible semi-circles, corresponding to the interfacial charge transfer resistance of 1.34, 1.22, 0.77 and 0.72Ω for PANI/CF, PANI/OCF, PANI/AFCF and PANI/ATFCF, respectively. The 45° sloped portion of the Nyquist plots over the low frequency region is related to the Warburg resistance from ion diffusion/transport in the electrolytes[13]. A shorter Warburg region implies a smaller Warburg resistance and enhanced ion movement. Among PANI and PANI/CFs composites, PANI/AFCF and PANI/ATFCF composite electrodes had the largest slope in the low frequency region, demonstrating small Warburg region as well as Warburg resistance, indicating that covalent connections between CF and PANI improved the ion diffusion. Long-term cycling stability of the electrode materials is a key index in supercapacitor. **Figure 5B** shows the capacitance retention of the electrodes during 1500 consecutive CV cycles at a scan rate of 100 mV s^{-1}. After 1500 cycles, the capacitance retentions of PANI, PANI/CF, PANI/OCF, PANI/AFCF, and PANI/ATFCF are 42.52%, 72.59%, 76.34%, 82.19%, and 84.19%, respectively. The results indicated that the four composite electrodes had high cycling stability in comparison with PANI. In particular, the covalent grafting PANI/AFTF and PANI/ATFTF composites had better cyclic stability than non-covalent composites.

Some points can be obtained from the above results. First, the incorporation of CF significantly improved the performance of PANI when using as supercapacitor electrodes. Secondly, surface functionalization of CF enhanced the interactions between PANI and CF, further improving the performance. Most importantly, the morphology and electrochemical performance of the PANI/CFs can be effectively controlled by the structural design of functional groups of CF. In PANI/OCF composites, PANI mainly had interactions with CF via hydrogen bonding, while covalent connections existed in PANI/AFCF and PANI/ATFCF composites. The covalent amino groups on CF surface can effectively guide the PANI growth, thus ordered nanostructures were prepared in PANI/AFCF and PANI/ATFCF, while disordered nanostructures in PANI/OCF. Depending on the distribution and directions of amino groups, nanowire arrays of PANI were obtained in PANI/AFCF and petal-like nanosheets in PANI/ATFCF. The strong covalent interactions and ordered nanostructures were beneficial in charge transfer on the interface and improved the electrochemical properties, Moreover, they also significantly improved the mechanical properties of the composites, effectively preventing the chain entanglement and collapse of PANI during the charge-discharge process, and even reducing the damage of PANI molecular chains. Consequently, the long-term cycling stability was obtained in covalently modified PANI/CF composites. The better performance of PANI/ATFCF than PANI/AFCF may be attributed to the more conjugated structure of the linking chains[28] (**Figure 1**), and the characteristic petal-like nanostructures of PANI, indicative of the significance in structural design of CF functionalization.

It is noting that the effect of surface modification on the electrochemical properties of CF itself is negligible (Figure S3). Moreover, though PANI content may influence the specific capacitance of composite materials, it isn't a key role here. PANI/OCF has a larger PANI content of 4.3% than PANI/CF, their difference of the specific capacitance is only 20.7 F/g. Conversely, PANI/AFCF has a larger PANI content of 3.3% than PANI/OCF, their difference of the specific capacitance is 62.5 F/g; PANI/ATFCF has a larger PANI content of 1.0% than PANI/AFCF, their difference of the specific capacitance is 50.6 F/g. These results demonstrate the importance of the synergistic effect of PANI and CF.

4. Conclusions

Three kinds of PANI/functionalized CF composite materials were prepared and their electrochemical performance in the application of supercapacitor electrodes was investigated. All the PANI/CF composites showed high electrochemical capacitance, together with excellent rate capability and good cycling stability. The morphologies and electrochemical performance of PANI/CFs hybrid materials strongly depended on the structural design of functional groups on the functionalized CF. Covalent connections between PANI and CF facilitated ordered nanostructures, resulting in even better performance. It is expected that the conclusions here can be also applied to other carbon based composite materials for supercapacitor electrode materials.

Acknowledgements

This research was financially supported bythe National Natural Science Fund of China (Grant Nos. 21471030，21271040 and 21171034), Shanghai Municipal Natural Science Foundation for Youths (No.12ZR144100) and "Chen Guang" project (No.12CG37) supported by Shanghai Municipal Education

Commission and Shanghai Education Development Foundation.

Notes and references

1. L. L. Zhang and X. S. Zhao, *Chem. Soc. Rev.*, 2009, **38**, 2520.
2. S. Bose; T. Kuila; A. K. Mishra; R. Rajasekar; N. H. Kim and J. H. Lee, *J. Mater. Chem.*, 2012, **22**, 767.
3. G. A. Snook; P. Kao and A. S. Best, *J. Power Sources*, 2011, **196**, 1.
4. G. Q. Ning; T. Y. Li; J. Yan; C. G. Xu; T. Wei and Z. J. Fan, *Carbon*, 2013, **54**, 241.
5. M. Li; Y. Q. Zhang and Y. K. Liu, *J. Mater. Sci-mater El*, 2014, **25**, 3509.
6. H. Kuang; Q. Cao; X. Y. Wang; B. Jing; Q. Wang and L. Zhou, *J. Appl. Polym. Sci.*, 2013, **130**, 3753.
7. S. Chatterjee; R. K. Layek and A. K. Nandi, *Carbon*, 2013, **52**, 509.
8. M. M. Sk; C. Y. Yue and R. K. Jena, *RSC Adv.*, 2014, **4**, 51887.
9. F. R. Jiang; W. Y. Li; R. J. Zou; Q. Liu; K. B. Xu; L. An and J. Q. Hu, *Nano Energy*, 2014, **7**, 72.
10. E. Frackowiak and F. Beguin, *Carbon*, 2001, **39**, 937.
11. W. W. Liu; X. B. Yan; J. T. Chen; Y. Q. Feng and Q. J. Xue, *Nanoscale*, 2013, **5**, 6053.
12. D. W. Wang; F. Li; J. P. Zhao; W. C. Ren; Z. G. Chen; J. Tan; Z. S. Wu; I. Gentle; G. Q. Lu and H. M. Cheng, *ACS Nano*, 2009, **3**, 1745.
13. Y. Wang; Z. Q. Shi; Y. Huang; Y. F. Ma; C. Y. Wang; M. M. Chen and Y. S. Chen, *J. Phys. Chem. C*, 2009, **113**, 13103.
14. J. J. Xu; K. Wang; S. Z. Zu; B. H. Han and Z. X. Wei, *ACS Nano*, 2010, **4**, 5019.
15. N. A. Kumar; H. J. Choi; Y. R. Shin; D. W. Chang; L. M. Dai and J. B. Baek, *ACS Nano*, 2012, **6**, 1715.
16. M. A. Q. Xue; F. W. Li; J. Zhu; H. Song; M. N. Zhang and T. B. Cao, *Adv. Funct. Mater.*, 2012, **22**, 1284.
17. F. Zhang; T. F. Zhang; X. Yang; L. Zhang; K. Leng; Y. Huang and Y. S. Chen, *Energ. Environ. Sci.*, 2014, **7**, 3086.
18. A. Khosrozadeh; M. Xing and Q. Wang, *Appl. Energ.*, 2015, **153**, 87.
19. Y. Liu; Y. Ma; S. Y. Guang; H. Y. Xu and X. Y. Su, *J. Mater. Chem. A*, 2014, **2**, 813.
20. C. P. Fonseca; D. A. L. Almeida; M. R. Baldan and N. G. Ferreira, *Chem. Phys. Lett.*, 2011, **511**, 73.
21. X. B. Yan; Z. X. Tai; J. T. Chen and Q. J. Xue, *Nanoscale*, 2011, **3**, 212.
22. M. K. Liu; S. X. He; W. Fan; Y. E. Miao and T. X. Liu, *Compos. Sci. Technol.*, 2014, **101**, 152.
23.Q. Cheng; J. Tang; J. Ma; H. Zhang; N. Shinya and L. C. Qin, *J. Phys. Chem. C*, 2011, **115**, 23584.
24. P. P. Yu; Y. Z. Li; X. Y. Yu; X. Zhao; L. H. Wu and Q. H. Zhang, *Langmuir*, 2013, **29**, 12051.
25. P. P. Yu; Y. Z. Li; X. Zhao; L. H. Wu and Q. H. Zhang, *Langmuir*, 2014, **30**, 5306.
26. J. W. An; J. H. Liu; Y. C. Zhou; H. F. Zhao; Y. X. Ma; M. L. Li; M. Yu and S. M. Li, *J. Phys. Chem. C*, 2012, **116**, 19699.
27. T. Morishita; Y. Soneda; H. Hatori and M. Inagaki, *Electrochim Acta*, 2007, **52**, 2478.
28. J. H. Liu; J. W. An; Y. C. Zhou; Y. X. Ma; M. L. Li; M. Yu and S. M. Li, *ACS Appl. Mater. Inter.*, 2012, **4**, 2870.

Graphical Abstract